




Article

Preparation of layered double hydroxide films using an electrodeposition and subsequent crystal growth method

Noriyuki Sonoyama* , Shizuka Yamada, Tomoki Ota, Haruna Inagaki, Patrick K. Dedetemo and Satoshi Yoshida
Department of Life and Applied Chemistry, Nagoya Institute of Technology, Gokiso-cyo, Showa-ku, Nagoya 466-8555, Japan

Abstract

The surface coating of a gas reaction electrode with layered double hydroxides (LDHs) featuring various electrode catalyst activities was prepared *via* electrodeposition and the subsequent crystal growth of LDHs. LDH formation was confirmed by X-ray diffraction and Raman scattering measurements after subsequent crystal growth on respective electrodeposited precursor films in Ni-Fe and Zn-Al LDH systems. However, the crystal growth of LDHs in Ni-Mn and Cu-Mn systems was observed on the Mg-Al LDH-electrodeposited films. LDH films were also deposited on the surface of a carbon paper electrode with a rugged surface *via* electrodeposition and subsequent crystal growth. Using the prepared LDH-coated carbon paper electrodes, the electrode catalytic activity for the oxygen reduction reaction (ORR) was examined. For Ni-Mn, Ni-Al and Ni-Fe LDH-coated carbon paper electrodes, the threshold voltages of the ORR decreased. Hence, the LDHs electrodeposited on a gas reaction electrode have high electrochemical catalytic activity for the ORR.

Keywords: coating on a porous electrode, electrode catalyst for oxygen reduction, electrodeposition, layered double hydroxide (LDH), subsequent crystal growth

(Received 7 May 2021; revised 18 January 2022; Accepted Manuscript online: 23 February 2022; Associate Editor: Huaming Yang)

Layered double hydroxides (LDHs), expressed by the general formula $(M^{II}_x M^{III}_{1-x}(\text{OH})_2)(A^{m-})_{x/m}$, are hydrotalcite-like materials with a structure based on brucite (Morales *et al.*, 2005; Guo *et al.*, 2010). The brucite layers are positively charged because of the partial substitution of M^{II} cations by M^{III} cations, and A^{m-} anions are inserted between the layers to neutralize the total charge using specific amounts of water molecules. Various chemical functions of LDHs arising from their characteristic structure have been reported, e.g. as catalysts (Cavani *et al.*, 1991; Ocelli & Robson, 1992), anion exchangers (Bish, 1980; Miyata, 1983; Ulibarri *et al.*, 1995) and anion conductors (Furukawa *et al.*, 2011; Miyazaki *et al.*, 2013). Recently, the electrochemical properties of LDHs have been investigated actively for their application as cathode materials in nickel batteries (Hu *et al.*, 2013, 2015; Yan & Yang, 2016), as precursors for lithium battery anode materials (Quan *et al.*, 2013a, 2014; Sonoyama *et al.*, 2021) and as electrode catalysts with gaseous reactants such as oxygen and hydrogen (Song & Hu, 2014; Trotochaud *et al.*, 2014; Liu *et al.*, 2017). Among these, active electrode materials for gaseous reactants find applications in sensors, fuel cell electrodes and air-based batteries. For application in a gas reaction electrode, the electrode catalyst should be uniformly supported on the surface of a porous substrate. To coat LDHs on porous materials, the main approaches used are the hydrothermal method (Cai *et al.*, 2015; Liang *et al.*, 2015) and the nanosheet deposition method (O'Leary *et al.*, 2002; Ma *et al.*, 2006, 2015). In the hydrothermal method, LDHs are directly synthesized on the surface of the

electrode. However, in this method, the substrate materials should be stable under hydrothermal conditions. In the nanosheet deposition method, nanosheets obtained *via* the layer-by-layer separation of LDHs are dispersed in solutions and allowed to permeate the porous materials, which are then dried. This method requires considerable time and effort, and a uniform coating on porous electrodes is difficult to achieve.

Electrodeposition is a well-known and efficient method for coating the surface of electronic conducting materials. Our research group has reported previously the electrodeposition of metal oxides on the surfaces of gold and carbon substrates as precursors of lithium-ion battery cathode materials (Quan *et al.*, 2013b; Sonoyama *et al.*, 2016). The advantage of the electrodeposition method is that it allows for uniform coating even on the rugged surfaces because deposition occurs over all parts of the electrode surface that are in contact with the electrolyte solution. Uniform LDH film formation on the surfaces of substrates would be beneficial for obtaining electrodes with fine catalytic activity, materials with improved optical characteristics *via* semiconductor surface coating and materials that are suitable for water treatment. The electrodeposition of several types of LDHs has been reported previously (Indira *et al.*, 1994; Scavetta *et al.*, 2007, 2009, 2012; Obayashi *et al.*, 2012). The deposition of LDHs mainly includes the following steps: hydrogen formation is induced at the surface of a cathode dipped in an electrolyte solution containing M^{II} and M^{III} ions with specific counteranions *via* the application of a current. This causes a partial increase in the pH of the electrolyte at the surface of the substrate due to proton consumption. Thin LDH films are deposited on the surface of the cathode. At the surface of the counterelectrode, mainly oxygen is formed. In the process of electrodeposition, few types of high-crystallinity LDH films can be obtained (Indira *et al.*, 1994) because limited crystal

*E-mail: sonoyama@nitech.ac.jp

Cite this article: Sonoyama N, Yamada S, Ota T, Inagaki H, Dedetemo PK, Yoshida S (2021). Preparation of layered double hydroxide films using an electrodeposition and subsequent crystal growth method. *Clay Minerals* 56, 284–291. <https://doi.org/10.1180/clm.2022.8>

growth time is available for the electrodeposition process. Certain specific types of LDHs are reported as exceptions, such as Zn-Al (Scavetta *et al.*, 2009) and Mn-Al LDHs (Obayashi *et al.*, 2012). In the present study, we attempted the synthesis of several types of LDH films on the surfaces of flat gold and rugged carbon paper electrodes using a simple and unified method: the electrodeposition of seed LDH crystals and subsequent crystal growth (homo-crystal growth). Several types of thin LDH films cannot be obtained *via* homo-crystal growth; therefore, crystal growth of a different kind of LDH on the surface of a different base LDH-electrodeposited film (hetero-crystal growth) was also attempted. The syntheses of the following combinations of LDHs were attempted in the present study, and the reasons for their synthesis are also listed:

- (1) Mg-Al LDH and Ni-Al LDH: their electrodeposition is facile and the LDH films obtained are applicable seed crystals of other LDHs.
- (2) Ni-Fe LDH, Ni-Mn LDH and Cu-Mn LDH: these LDHs are expected to be fine catalysts or electrodes with good electrocatalytic activities due to their loading of two types of transition metal ions.
- (3) Zn-Al LDH: this LDH is also expected to act as a semiconductor material *via* simple sintering.

LDH surface coating was also attempted on the surface of the carbon paper with a rugged surface structure, and the electrochemical performance of the LDH-coated carbon paper as a gas reaction electrode for the oxygen reduction reaction (ORR) was examined.

Experimental

All deposition processes were carried out under the following conditions: films were deposited on the surface of the cathodes, with a flat gold substrate (10 mm × 10 mm, thickness = 0.2 mm) or with carbon paper (TGP-H-120, Toray, Japan; 10 mm × 10 mm, $t = 0.34$ mm) with a rugged surface as the substrate, at a constant current of 17 mA using a gold sheet as the counterelectrode. The electrolyte solution contained the nitrate compound of M^{II} and M^{III} ions and NaNO_3 at concentrations of 0.05, 0.025 and 1.0 M, respectively. The total electrolysis time was 10 min. Variation of the M^{II} - M^{III} ions was studied *via* combinations of Ni-Al, Ni-Mn, Ni-Fe, Cu-Mn and Zn-Al. All chemicals were purchased from Kishida Kagaku (Japan; Guaranteed Reagent grade). After electrodeposition, crystal growth of the LDH film was attempted. The electrodeposited films were dipped in a solution with the same components as the electrodeposition bath. After adjusting the pH of the solution to 9.0 *via* the addition of NaOH solution, the films were stored at 80°C under stirring for 3 days. For Mg-Al and Ni-Al LDH films, crystal growth was attempted to prepare the substrate (seed crystals) for other system baths, such as Ni-Mn and Cu-Al.

The films obtained were characterized using X-ray diffraction (XRD; Ultima IV, Rigaku, Japan) with Cu- $K\alpha$ radiation. The monochromatization of the diffracted X-rays was carried out using a Soller slit and a light receiving slit, and the diffracted X-rays were detected using a scintillation counter. The morphology of the film surface was observed using scanning electron microscopy (SEM) and energy-dispersive spectroscopy (EDS; JSM-6010LA, JEOL, Japan). The measurement conditions for EDS were as follows: measurement time = 50 s, acceleration voltage = 8 kV, measurement area = 0.6 mm × 0.4 mm (maximum).

The molecular ratios of the transition metal ions in the films obtained were determined using EDS.

The electrochemical properties of the films obtained were examined using linear sweep voltammetry with film-deposited carbon paper, Pt wire and Ni wire as the working electrode, counter-electrode and quasi-reference electrode, respectively. Measurements were carried out in a 6 M KOH aqueous solution with oxygen bubbling using a potentiostat (HZ-7000, Hokuto, Japan) and a gas reaction cell (ECC-Air, EL-CELL, Germany).

Results and discussion

The diffraction peak positions of 003 and 006 of the Mg-Al LDH in the Inorganic Crystal Structure Database (ICSD; #81963) are shown using blue lines in Fig. 1. A very weak and broad diffraction peak was observed at $\sim 11^\circ 2\theta$, which could be assigned to the 003 diffraction of LDH for Ni-Al and Mg-Al systems. The peak at $\sim 12.5^\circ 2\theta$ observed for the Cu-Mn system was assigned to an impurity, which is discussed later. Other characteristic diffraction peaks of LDH were not obtained using the synthesis process employed in this study. For other systems, very weak peaks were observed corresponding to the 003 diffraction line for LDHs and suggesting the unsuccessful formation of LDH films. Figure 1b shows the XRD traces of the films after crystal growth. The 003 and 006 diffraction peaks at $11\text{--}12^\circ 2\theta$ and $23\text{--}24^\circ 2\theta$, respectively, were observed for the Ni-Al, Mg-Al, Ni-Fe and Zn-Al systems, but not for the Ni-Mn and Cu-Mn systems. Other diffraction peaks of LDH were not observed after the crystal-growth process. For the Ni-Al and Mg-Al systems, the 003 diffraction line, which was originally observed before homo-crystal growth, became more intense, and the 006 diffraction line, which was not observed in the electrodeposited films, was detected.

For the Ni-Fe and Zn-Al systems, the 003 and 006 diffraction lines that were not observed for the electrodeposited films were observed after the homo-crystal growth process. Moreover, an indeterminable amount of impurity (ZnO) was observed for the Zn-Al system. These results suggest that the small seed crystals of LDHs formed during the electrodeposition process grew in the subsequent homo-crystal growth process. The peak at $\sim 12.5^\circ 2\theta$ for the Cu-Mn system could be assigned to the impurity phase. The space group of the Cu-Mn LDH is different from that of the Mg-Al LDH (Zhang *et al.*, 2021). The reason for this is discussed below. Other characteristic diffraction peaks of LDH were not detected in this study.

Table 1 summarizes the interlayer diffraction peak positions, d spacings and ratios of M_1 and M_2 contents estimated from the EDS analyses. The differences in the peak positions and d spacings for the obtained LDHs are not significant. By contrast, differences were observed in the M_1/M_2 ratios. For the Mn-Al and Ni-Al systems, the M_1/M_2 ratios were almost identical, but their values did not agree with the M_1/M_2 ratio in the electrolyte solution. During the electrodeposition process, LDH is formed due to the rapid pH increase at the surface of the electrode induced by the conversion of protons to hydrogen. Due to this rapid crystal formation in a non-equilibrium state, an LDH with a stable composition is formed.

In the Zn-Al system, the M_1/M_2 ratio obtained was too large for LDH formation. This large M_1/M_2 ratio was due to the formation of the impurity phase, zinc oxide (ZnO), during the electrodeposition process. The ZnO formed during the electrodeposition process is evident in Fig. 1a. ZnO is formed easily due to the rapid increase in pH during the LDH synthesis process. During

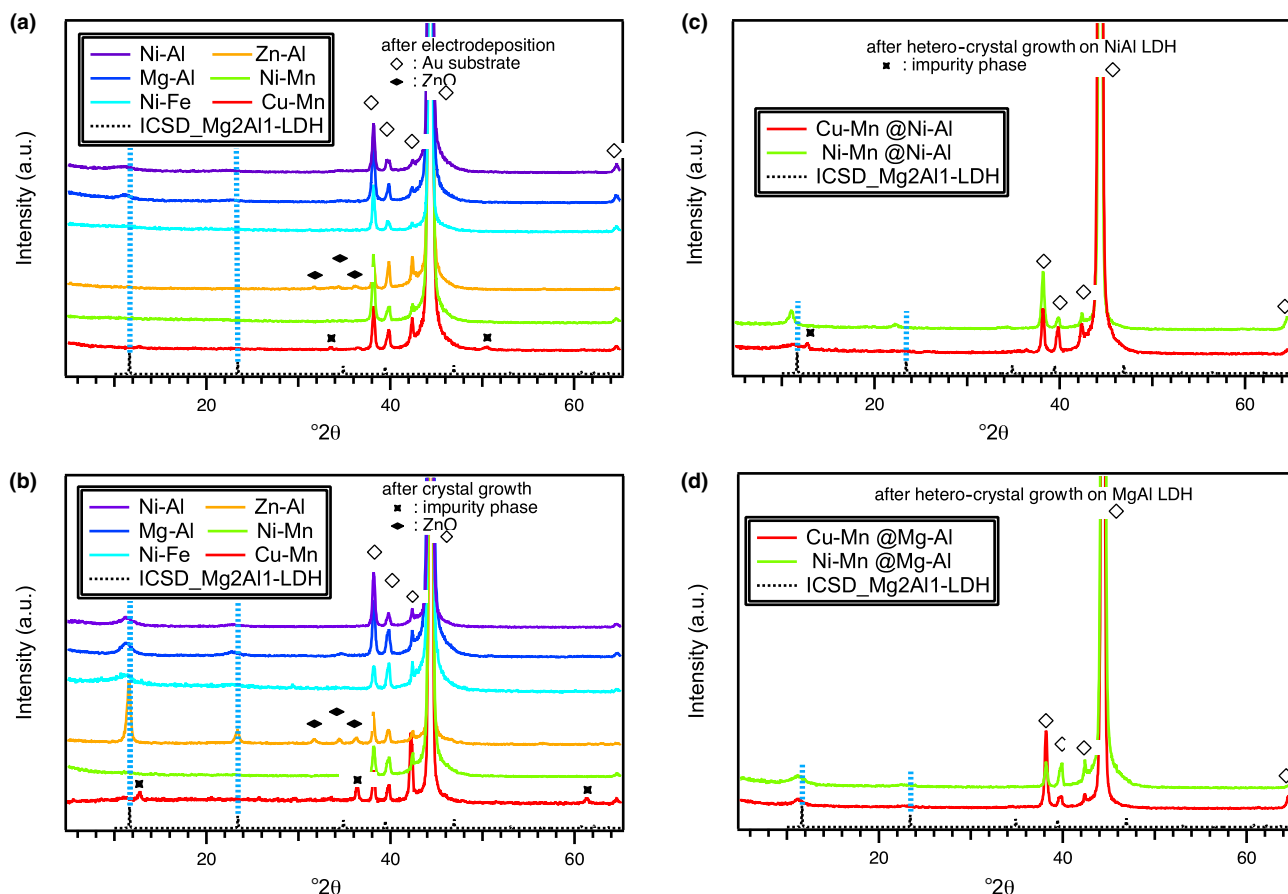


Fig. 1. XRD traces of the electrodeposited thin film on gold substrate: (a) before subsequent crystal growth, (b) after subsequent crystal growth, (c) after hetero-crystal growth on a thin Ni-Al LDH film and (d) after hetero-crystal growth on a thin Mg-Al LDH film. 'ICSD_Mg2Al1-LDH' refers to the XRD trace of Mg-Al LDH with a Mg/Al ratio of 2.0 in the ICSD database.

Table 1. The peak position of 003 diffraction lines, d spacings and $M_1^{\text{II}}/M_2^{\text{II}}$ ratios of various compound systems.

Compound system	Peak position of 003 diffraction line (°)	d spacing (Å)	$M_1^{\text{II}}/M_2^{\text{II}}$ ratio
Mg-Al	11.5	7.69	1.43
Ni-Al	11.5	7.69	1.46
Zn-Al	11.7	7.56	5.30
Ni-Fe	11.5	7.69	1.49
Ni-Mn/Mg-Al LDH	11.2	7.89	-
Ni-Mn/Ni-Al LDH	11.1	7.96	-
Cu-Mn/Mg-Al LDH	11.2	7.89	-

electrodeposition, the pH at the electrode surface will increase rapidly with the hydrogen formation that accompanies the consumption of protons. This significant increase in pH induces the formation of ZnO.

For the Ni-Mn and Cu-Mn systems, the M_1/M_2 ratios were 16.6% and 14.8%, respectively (after homo-crystal growth; not shown in Table 1). These results suggest that Mn^{3+} is present to only a very small degree in the electrodeposited film obtained. The reason for this unsuccessful LDH formation is unclear. One possibility is that the dissolution of Mn^{3+} might dissolve in the electrolyte solution (Hirayama *et al.*, 2010).

Figure 2 shows SEM images and EDS atomic mapping images of the substrate surface after electrodeposition for the Ni-Fe system.

Small particles covering the surface of the substrate are clearly evident. Furthermore, from the EDS atomic mapping images, it can be seen that the Ni^{2+} and Fe^{3+} ions are distributed uniformly over the same area, suggesting that a solid solution of binary metal compounds constitute the electrodeposition bath. Figure 2c shows a SEM image of the substrate surface after electrodeposition for the Zn-Al system. Particles of various shapes were deposited on the substrate, and these particles seem to be those of the ZnO impurity.

Raman spectra of the electrodeposited films in the Ni-Fe and Zn-Al systems are shown in Fig. 3. A scattering band observed at 1100 cm^{-1} was assigned to ν_1 mode scattering for LDHs (De Faria *et al.*, 1998; Rives, 2001). For the Ni-Fe and Zn-Al systems, well-defined interlayer diffraction peaks of LDH were not observed after the electrodeposition process. The Raman spectra indicated small seed crystal formation of Ni-Fe and Zn-Al LDHs during the electrodeposition process. In other words, the crystal growth of Ni-Fe and Zn-Al LDHs proceeds only to a very small degree during electrodeposition. The crystal growth of LDHs depends on many factors, such as the deposition pH values, the electron conductivity of the deposited LDHs and OH^- ion mobility. For such systems, the seed crystals of LDHs grow only to a very small degree during electrodeposition, and the subsequent crystal-growth process would be effective for the synthesis of thin LDH films.

Figure 1c,d shows the XRD traces of the films after hetero-crystal growth in the Cu-Mn and Ni-Mn solution baths on the electrodeposited Ni-Al LDH and Mg-Al LDH films. For the

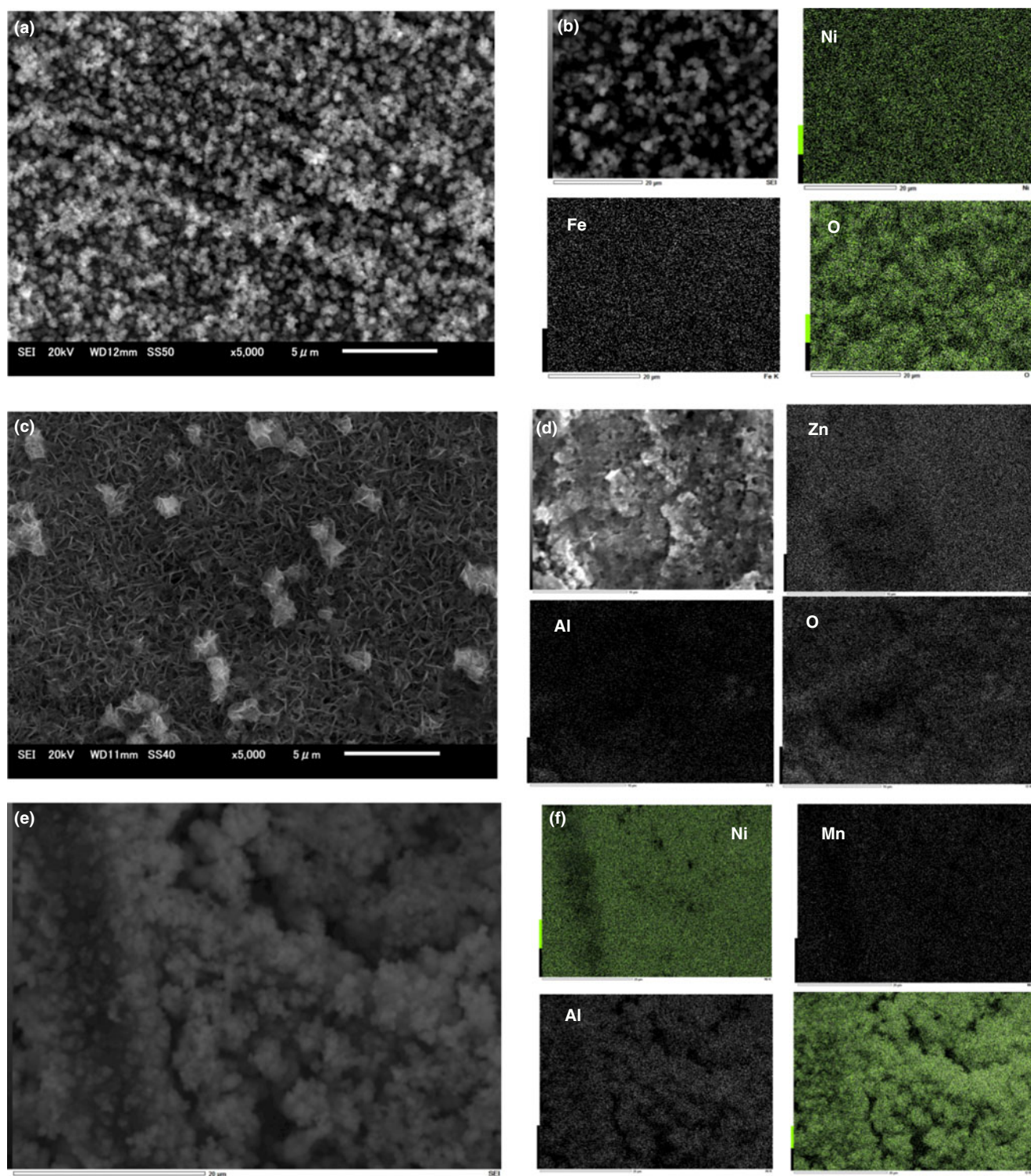


Fig. 2. SEM image and EDS atomic mapping images of substrate surfaces after electrodeposition in the: (a,b) Ni-Fe and (c,d) Zn-Al systems, respectively. (e) SEM image and (f) EDS atomic mapping images of the Ni-Mn LDH/Ni-Al LDH hybrid film after the hetero-crystal growth process.

Ni-Mn system, an apparent increase in the 003 diffraction was observed for both the Ni-Mn/Ni-Al LDH and Ni-Mn/Mg-Al LDH films, suggesting the growth of Ni-Mn LDH on the surface of Ni-Al LDH and Mg-Al LDH.

Figure 2e,f shows a SEM image and EDS atomic mapping of the Ni-Mn LDH/Ni-Al LDH hybrid film after the hetero-crystal

growth process. Particles $<1\ \mu\text{m}$ in size appear to cover the surface. The EDS atomic mapping images confirm that Ni, Mn and O are distributed over the same regions, indicating the formation of Ni-Mn LDH. Moreover, Al, which is a component of the base film, is observed on the surface of the film. The detection of Al might have been caused by the translation of X-rays through

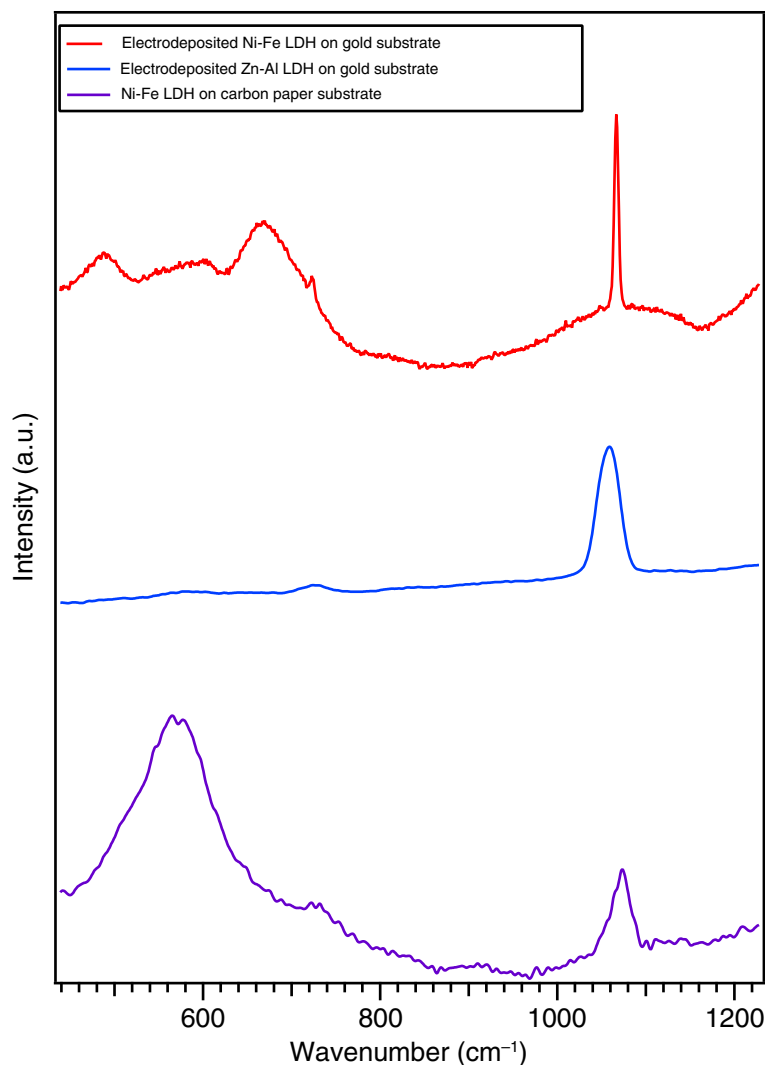


Fig. 3. Raman spectra for electrodeposited films on the gold substrate in the Ni-Al and Zn-Al systems after electrodeposition and for film deposition on the carbon paper substrate in the Ni-Fe system after homo-crystal growth.

the surface-covering Ni-Mn LDH layer over the Ni-Al LDH layer. The molecular ratios of these elements are summarized in Table 2. The composition of the thin film was estimated to be $\text{Ni}_{1.7}\text{Mn}_{0.5}\text{Al}_{0.5}(\text{OH})_{4.8}(\text{NO}_3)_{0.57}$. This composition is determined from the average of the surface Ni-Mn LDH layer and the underlying Ni-Al LDH layer contents.

The XRD traces for the Cu-Mn films over Ni-Al LDH and Mg-Al LDH films hetero-grown in the Cu-Mn bath are shown in Fig. 1c,d. A peak of the impurity phase that was observed in Fig. 1b appeared for the Ni-Al LDH seed layer after crystal growth. For the Mg-Al LDH seed crystal shown in Fig. 1d there is an apparent increase in the intensity of the interlayer diffraction, which agrees with the nature of the diffraction peak reported by Zhang *et al.* (2021). At present, the reason for this inactivity of the crystal growth of Cu-Mn LDH on Ni-Al LDH seed crystals is not clear. However, a weak diffraction peak can be observed at the interlayer diffraction position for the Cu-Mn LDH/Ni-Al LDH system (Fig. 1c), suggesting the simultaneous crystal growth of Cu-Mn LDH and the impurity phase. The molecular ratios of Cu-Mn LDH/Mg-Al LDH are shown in Table 2. The M_1/M_2 ratio of Cu-Mn LDH is estimated to be 2.05, which is more suitable for a LDH than the value of 14.8 obtained *via* homo-crystal growth (Fig. 1b).

Table 2. Atomic contents of the LDH systems after the hetero-crystal growth process.

<i>Ni-Mn/Ni-Al LDH system (base LDH mol.% Ni:Al = 18.0:8.2)</i>						
Element	Al	Mn	Ni	O	Total	
Mol.%	4.1	4.9	15.6	75.4	100	
<i>Ni-Mn/Mg-Al LDH system (base LDH mol.% Mg:Al = 10.1:5.4)</i>						
Element	Mg	Al	Mn	Ni	O	Total
Mol.%	12.8	5.6	1.9	3.0	76.7	100
<i>Cu-Mn/Mg-Al LDH system (base LDH mol.% Mg:Al = 8.1:7.2)</i>						
Element	Mg	Al	Mn	Cu	O	Total
Mol.%	6.5	6.1	3.4	7.0	77.0	100

Figure 4a shows a transmission electron microscopy image of the Ni-Mn LDH crystal grown on an electrodeposited Ni-Al film. A needle-shaped crystal with a different shape from that of the base crystal (plane-shaped) was formed. This suggests that the hetero-crystal growth does not proceed *via* epitaxial crystal growth. It is suggested that once the second layer of crystals begins to be deposited on the base crystal, the subsequent crystal growth proceeds in various directions in addition to the original direction.

To fabricate a gas reaction electrode supported with an electrode catalyst (LDH), it is necessary to homogeneously coat catalyst compounds over the surface of the porous electrode. However,

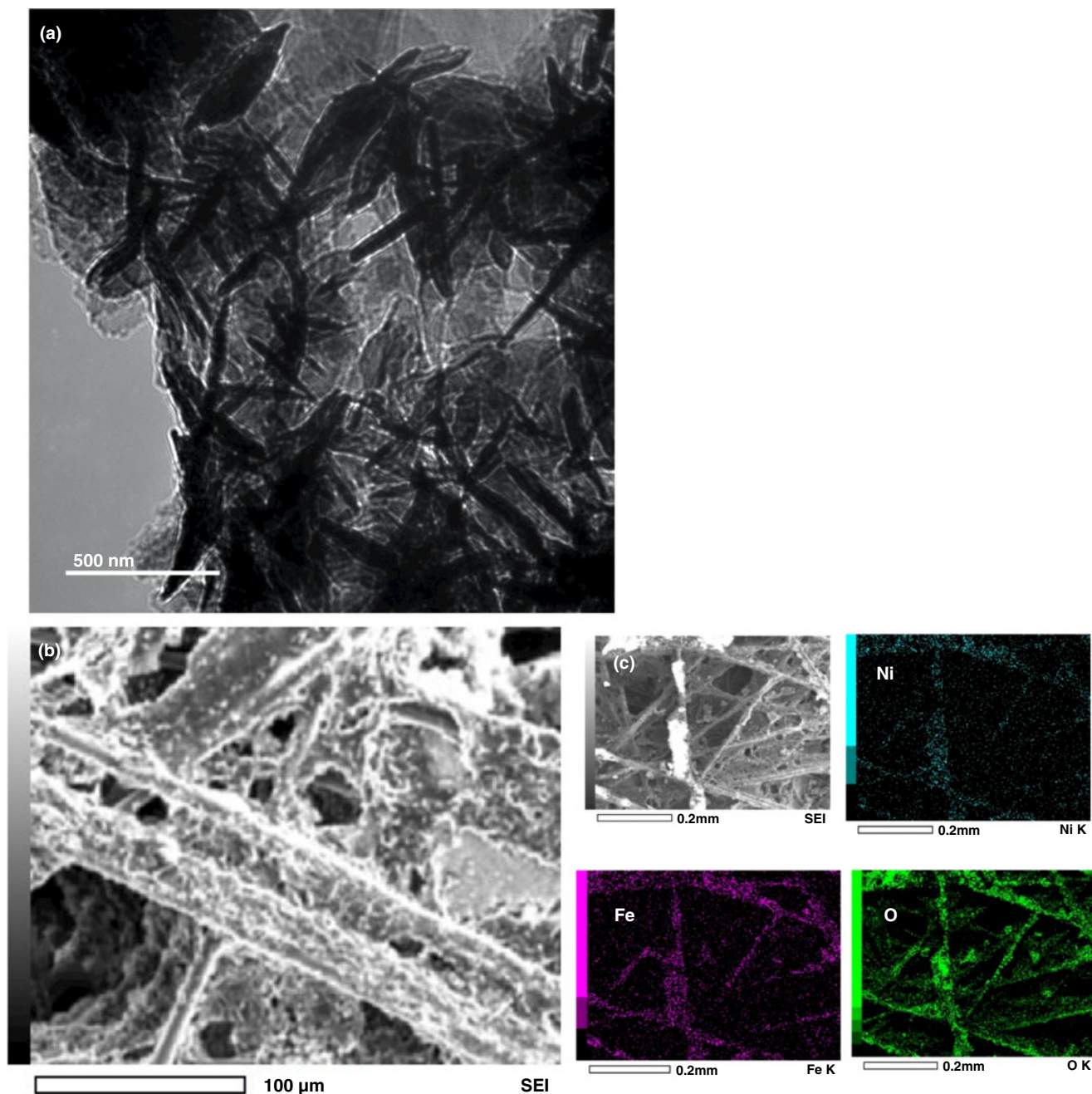


Fig. 4. (a) Transmission electron microscopy image of Ni-Mn LDH on Ni-Al LDH. (b) SEM image and (c) EDS atomic mapping images of a Ni-Fe LDH film on a carbon paper substrate.

coating LDHs on the surfaces of porous materials is difficult. One of the most popular methods of surface coating is nanosheet coating (O'Leary *et al.*, 2002; Ma *et al.*, 2006). LDHs can be separated layer by layer to disperse LDH nanosheets in a solution, which can be coated over the electrode by dipping it in this dispersion. However, achieving a homogeneous coating on a porous surface is difficult, and some additives, such as dodecyl benzene sulfonate (DBS) anions, which are the typical addition agents used to form LDH nanosheet dispersions, are also loaded onto the electrodes. DBS has low reactivity for sub-reactions. However, the presence of DBS on the surface may reduce the reactivity of the electrode due to its low electrical conductivity and large surface area. Electrodeposition and subsequent crystal growth represent a simple

and appropriate method for covering a porous electrode surface with LDHs because electrodeposition occurs at the surface of the electrode that is in contact with the electrolyte solution, which is appropriate for coating an electrode catalyst or electrode active materials over the surface. In a previous paper, we reported the coating of LiCoO_2 nanosized particles on the surface of a rugged electrode (Sonoyama *et al.*, 2016). In the present study, the electrodeposition of LDHs on the surface of a rugged carbon paper electrode was attempted using electrodeposition and subsequent crystal growth.

For thin films deposited on the rugged electrode, no XRD profile could be obtained because a flat surface is necessary for XRD. Figure 4b shows a SEM image of a carbon paper electrode surface after Ni-Fe LDH synthesis *via* electrodeposition and subsequent

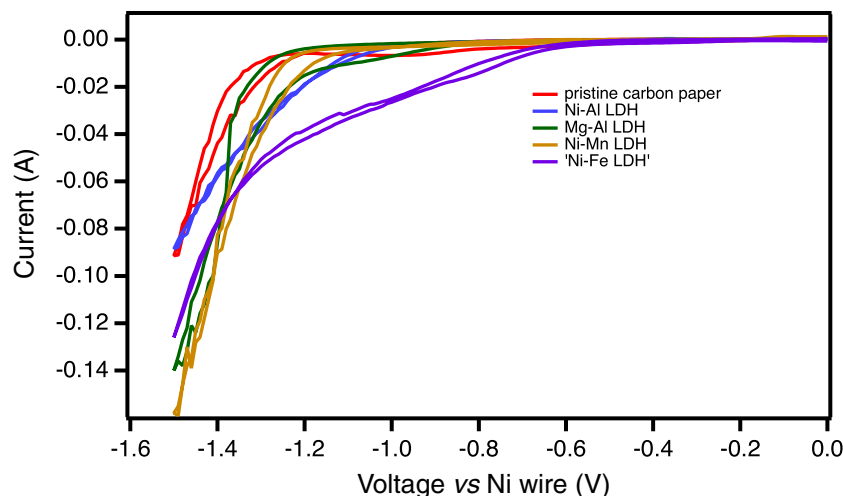


Fig. 5. Cyclic voltammograms for carbon paper electrodes coated with various LDHs under constant oxygen flow.

crystal growth. LDH particles with sizes <100 nm were confirmed to be deposited on the surface of the carbon paper. EDS atomic mapping images of the Ni-Fe LDH-deposited surface are shown in Fig. 4c. The distribution of these two metals in the same area suggests the formation of a solid solution. The characteristic band at 1100 cm^{-1} in the Raman scattering spectra shown in Fig. 3 also indicates the successful formation of LDHs on the carbon paper electrodes *via* electrodeposition and subsequent crystal growth.

To examine the reaction activity of LDH-coated carbon paper electrodes with gaseous compounds, the ORR activity was estimated using cyclic voltammetry (CV) under constant oxygen flow. The CV curves for various LDH-coated carbon paper electrodes are shown in Fig. 5. For Ni-Fe LDH-, Ni-Mn LDH- and Ni-Al LDH-coated electrodes, a decrease in the polarized potential with an increase in the current for the ORR was observed, which contrasts with the pristine and Mg-Al LDH-coated electrodes that have no electrical conductivity. This result demonstrates the catalytic activity of the LDH-coated electrodes for oxygen reduction.

Conclusion

In the present study, it was demonstrated that electrodeposition and subsequent crystal growth represent a useful method for achieving various LDH coatings on the surfaces of rugged-surface electrodes. This method can be applied for the preparation of gas-diffusion electrodes that are suitable for use in ORR.

References

- Bish D.L. (1980) Anion-exchange in takovite: applications to other hydroxide minerals. *Bulletin de Mineralogie*, **103**, 170–175.
- Cai X., Shen X., Ma L., Ji Z., Xu C. & Yuan A. (2015) Solvothermal synthesis of NiCo-layered double hydroxide nanosheets decorated on RGO sheets for high performance supercapacitor. *Chemical Engineering Journal*, **268**, 251–259.
- Cavani F., Trifiro F. & Vaccari A. (1991) Hydrotalcite-type anionic clays: preparation, properties and applications. *Catalysis Today*, **11**, 173–301.
- De Faria D.L.A., Constantino V.R.L., Baldwin K.J., Batchelder D.N., Pinnavaia T.J. & Chibwe M. (1998) Raman microspectroscopy of phthalocyanine intercalates: tetrasulfonated cobalt and nickel phthalocyanines in layered double hydroxide. *Journal of Raman Spectroscopy*, **29**, 103–108.

- Furukawa Y., Tadanaga K., Hayashi A. & Tatsumisago M. (2011) Evaluation of ionic conductivity for Mg-Al layered double hydroxide intercalated with inorganic anions. *Solid State Ionics*, **192**, 185–187.
- Guo X., Zhang F., Evans D.G. & Duan X. (2010) Layered double hydroxide films: synthesis, properties and applications. *Chemical Communications*, **46**, 5197–5210.
- Hirayama M., Ido H., Kim K.S., Cho W., Tamura K., Mizuki J. & Kanno R. (2010) Dynamic structural changes at LiMn_2O_4 /electrolyte interface during lithium battery reaction. *Journal of the American Chemical Society*, **132**, 15268–15276.
- Hu J., Lei G., Lu Z., Liu K., Sang S. & Liu H. (2015) Alternating assembly of Ni-Al layered double hydroxide and graphene for high-rate alkaline battery cathode. *Chemical Communications*, **51**, 9983–9986.
- Hu M., Ji X., Lei L. & Lu X. (2013) The effect of cobalt on the electrochemical performances of Ni-Al layered double hydroxides used in Ni-M(H) battery. *Journal of Alloys and Compounds*, **578**, 17–25.
- Indira L., Dixit M. & Kamath P.V. (1994) Electrosynthesis of layered double hydroxides of nickel with trivalent cations. *Journal of Power Sources*, **52**, 93–97.
- Liang H., Meng F., Caban-Acevedo M., Li L., Forticaux A., Xiu L. *et al.* (2015) Hydrothermal continuous flow synthesis and exfoliation of NiCo layered double hydroxide nanosheets for enhanced oxygen evolution catalysis. *Nano Letters*, **15**, 1421–1427.
- Liu W., Bao J., Guan M., Zhao Y., Lian J., Qiu J. *et al.* (2017) Nickel-cobalt-layered double hydroxide nanosheet arrays on Ni foam as a bifunctional electrocatalyst for overall water splitting. *Dalton Transactions*, **46**, 8372–8376.
- Ma R., Liu Z., Li L., Iyi N. & Sasaki T. (2006) Exfoliating layered double hydroxides in formamide: a method to obtain positively charged nanosheets. *Journal of Materials Chemistry*, **16**, 3809–3813.
- Ma W., Ma R., Wang C., Liang J., Liu X., Zhou K. & Sasaki T. (2015) A superlattice of alternately stacked Ni-Fe hydroxide nanosheets and graphene for efficient splitting of water. *ACS Nano*, **9**, 1977–1984.
- Miyata S. (1983) Anion-exchange properties of hydrotalcite-like compounds. *Clays and Clay Minerals*, **31**, 305–311.
- Miyazaki K., Asada Y., Fukutsuka T., Abe T. & Bendersky L.A. (2013) Structural insights into ion conduction of layered double hydroxides with various proportions of trivalent cations. *Journal of Materials Chemistry A*, **1**, 14569–14576.
- Morales J., Sanchez L., Bijani S., Martinez L., Gabas M. & Ramos-Barrado J.R. (2005) Electrodeposition of Cu_2O : an excellent method for obtaining films of controlled morphology and good performance in Li-ion batteries. *Electrochemical and Solid-State Letters*, **8**, A159–A162.
- O'Leary S., O'Hare D. & Seeley G. (2002) Delamination of layered double hydroxides in polar monomers: new LDH-acrylate nanocomposites. *Chemical Communications*, **2002**, 1506–1507.
- Obayashi C., Ishizaka M., Konishi T., Yamada H. & Katakura K. (2012) Preparation of the electrochemically precipitated Mn-Al LDHs and their electrochemical behaviors. *Electrochemistry*, **80**, 879–882.

- Occelli M.L. & Robson H. (1992) *Expanded Clays and Other Microporous Solids*. Van Nostrand Reinhold, New York, NY, USA, 379 pp.
- Quan Z., Ni E., Hayashi S. & Sonoyama N. (2013a) Structure and electrochemical properties of multiple metal oxide nanoparticles as cathodes of lithium batteries. *Journal of Materials Chemistry A*, **1**, 8848–8856.
- Quan Z., Ni E., Ogasawara Y. & Sonoyama N. (2014) Electrochemical properties of nano-sized binary metal oxides as anode electrode materials for lithium battery synthesized from layered double hydroxides. *Solid State Ionics*, **262**, 128–132.
- Quan Z., Ohguchi S., Kawase M., Tanimura H. & Sonoyama N. (2013b) Preparation of nanocrystalline LiMn_2O_4 thin film by electrodeposition method and its electrochemical performance for lithium battery. *Journal of Power Sources*, **244**, 375–381.
- Rives V. (2001) *Layered Double Hydroxides: Present and Future*. Nova Publishers, New York, NY, USA, 439 pp.
- Scavetta E., Ballarin B., Corticelli C., Gualandi I., Tonelli D., Prevot V. *et al.* (2012) An insight into the electrochemical behavior of Co/Al layered double hydroxide thin films prepared by electrodeposition. *Journal of Power Sources*, **201**, 360–367.
- Scavetta E., Ballarin B., Gazzano M. & Tonelli D. (2009) Electrochemical behaviour of thin films of Co/Al layered double hydroxide prepared by electrodeposition. *Electrochimica Acta*, **54**, 1027–1033.
- Scavetta E., Mignani A., Prandstraller D. & Tonelli D. (2007) Electrosynthesis of thin films of Ni, Al hydrotalcite like compounds. *Chemistry of Materials*, **19**, 4523–4529.
- Song F. & Hu X. (2014) Exfoliation of layered double hydroxides for enhanced oxygen evolution catalysis. *Nature Communications*, **5**, 4477.
- Sonoyama N., Niki K., Koide A., Eguchi M., Ogasawara Y., Tsukada T. & Dedetemo P.K. (2021) Structure and reaction mechanism of binary Ni-Al oxides as materials for lithium-ion battery anodes. *Dalton Transactions*, **50**, 14176–14186.
- Sonoyama N., Tanimura H., Mizuno T., Ogasawara Y. & Quan Z. (2016) Preparation of LiCoO_2 thin film consisting of nanosize particles on carbon substrate with the rugged surface *via* electrodeposition. *Solid State Ionics*, **285**, 106–111.
- Trotochaud L., Young S.L., Ranney J.K. & Boettcher S.W. (2014) Nickel-iron oxyhydroxide oxygen-evolution electrocatalysts: the role of intentional and incidental iron incorporation. *Journal of the American Chemical Society*, **136**, 6744–6753.
- Ulibarri M.A., Pavlovic I., Hermosin M.C. & Cornejo J. (1995) Hydrotalcite-like compounds as potential sorbents of phenols from water. *Applied Clay Science*, **10**, 131–145.
- Yan J. & Yang Z. (2016) Based on the performance of hydrotalcite as anode material for a Zn-Ni secondary cell, a modification: PPY coated Zn-Al-LDH was adopted. *RSC Advances*, **6**, 85117–85124.
- Zhang Y., Lin Y., Huang Z., Jing G., Zhao H., Wu X. & Zhang H. (2021) CuMnAl-O Catalyst synthesized *via* pyrolysis of a layered double hydroxide precursor attains enhanced performance for benzene combustion. *Energy & Fuels*, **35**, 743–751.